Failure probability of regional flood defences

Kasper Lendering[1,a]

[1] *Delft University of Technology, Faculty of Civil Engineering and Geosciences, Delft, the Netherlands*

Abstract. Polders in the Netherlands are protected from flooding by primary and regional flood defence systems. During the last decade, scientific research in flood risk focused on the development of a probabilistic approach to quantify the probability of flooding of the primary flood defence system. This paper proposed a methodology to quantify the probability of flooding of regional flood defence systems, which required several additions to the methodology used for the primary flood defence system. These additions focused on a method to account for regulation of regional water levels, the possibility of (reduced) intrusion resistance due to maintenance dredging in regional water, the probability of traffic loads and the influence of dependence between regional water levels and the phreatic surface of a regional flood defence. In addition, reliability updating is used to demonstrate the potential for updating the probability of failure of regional flood defences with performance observations. The results demonstrated that the proposed methodology can be used to determine the probability of flooding of a regional flood defence system. In doing so, the methodology contributes to improving flood risk management in these systems.

1 Introduction

Historically the Netherlands have always had to deal with the threat of flooding, both along the major rivers, the coast and from heavy rainfall. The country consists of a large amount of reclaimed polders which typically lie below the surrounding water and are protected from flooding by primary and/or regional flood defences. Primary flood defences protect polders from the main flood hazards, examples are river dikes for protection against river floods and storm surge barriers for protection against storm surges. Regional flood defences protect polders from regional water, examples are embankments along polder drainage canals. Figure 1 shows an example of a regional flood defence in the Netherlands (on the left) and another along the 17th street canal in New Orleans (on the right).

Figure 1. Regional flood defence in the Netherlands (Rijkswaterstaat)

Until recently, the strength of the primary flood defences in the Netherlands was assessed with a deterministic approach that determined if the flood defence was strong enough to survive one maximum water level. During the last decade, scientific research in flood risk focused on the development of a probabilistic approach to assess the strength of the flood defence for all possible water levels. This approach was used to quantify the probability of failure and risk of flooding of all primary flood defences in the Netherlands in a project called 'Flood Risk of the Netherlands 2' [1,2]. Regional flood defences were not taken in to account in this project, even though there are several polders in the Netherlands at significant risk of flooding from regional water. The development of a probabilistic approach to quantify the probability of flooding of regional flood defence systems can contribute to more effective flood risk management in polders.

In this paper, we applied the probabilistic methods developed for the primary flood defences in the Netherlands to a system of regional flood defences to quantify the probability of flooding of this system. The application to the regional flood defence system requires several additions to account for different type of loads and flood defences. We will focus on earthen dikes that protect the polders from flooding from the drainage canals. This paper is based on a more extensive technical report; more information on the discussed framework and case study can be found in [3].

[a] Corresponding author: k.t.lendering@tudelft.nl

The paper is built up as follows. Section 2 describes the methodology proposed to quantify the probability of flooding of a regional flood defence system. In section 3, we apply the methodology to a case study in the Netherlands. Section 4 discusses the assumptions made and how the methodology can be optimized further. Conclusions regarding the methodology and case study results are given in paragraph 5, followed by recommendations for further research.

2 Flood probability assessment

2.1 System description

Polders often lay below the surrounding water level and are temporarily or permanently at risk of flooding from the surrounding water. Water enters polders through groundwater flow and/or rainfall. Excess water is drained to the surrounding water through a drainage canal system. Water is first collected in a collection of ditches from where it is pumped on to drainage canals. These canals serve as a temporary storage system before water is ultimately drained to the surrounding water, which may be a river, a lake or the sea. A schematized plan view of such a system is shown in Figure 2.

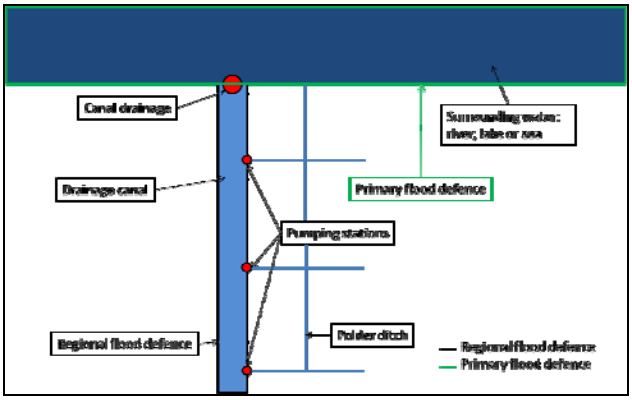

Figure 2. Plan view of a polder including the drainage system that contains three water levels: polder ditches, drainage canals the outside water

The drainage canals are enclosed by embankments that function as a regional flood defence. Traditionally, these regional flood defences were constructed from locally available soil in polders: this is often a mixture of clayey and peat material. Seepage to the surrounding polders is limited due to the low conductivity of the clayey / peat material used for construction of the regional flood defences. The title is set in bold 14-point Arial, flush left, unjustified. The first letter of the title should be capitalised with the rest in lower case. You should leave 35 mm of space above the title and 6 mm after the title.

2.2 General approach

Flood risk is described by the annual expected damage of flooding, which is found by multiplying the annual probability of flooding with the consequences of flooding (see equation 1). This paper focusses on quantifying the probability of flooding of a regional flood defence system. To this purpose, we will use the methods developed in the VNK-2 projec t[2]. An assessment of the consequences of flooding of regional flood defence system is beyond the scope of this paper, but is treated in the technical report [3].

$$Risk = Probability\ (yr\text{-}1) * Consequences\ (€) \qquad (1)$$

The considered regional flood defence system is divided in separate flood defence sections, each with similar strength properties, which allows independent modelling of sections. Following the division in sections, the system is divided in separate flood scenarios. A flood scenario is defined as a group of flood defence sections that will result in similar flooding irrespective of the location of failure within the considered group.

The probability of flooding of each scenario ($P_{f;scenario}$) is determined by combination of the probability of failure of each section ($P_{f;i}$) within the considered flood scenario. Failure is defined as breaching of the flood defence and occurs when the load (S) exceeds the resistance (R) of the flood defence. For example, a flood defence fails when the water level in the canal (i.e. the load) exceeds the retaining height of the flood defence (i.e. the resistance). Limit state functions (Z) are derived for the governing failure mechanisms of the considered flood defence. The general form of a limit state function is shown in equation 2, where the loads are described by the Solicitation and the strength by the Resistance. The probability of the considered failure mechanism is quantified by the probability that the limit state function is smaller than zero (equation 3).

$$Z = Resistance - Solicitation \qquad (2)$$

$$P_{f;i} = P(Z=0) = P(S>R) \qquad (3)$$

Fragility curves represent the cumulative density function of the strength (Fr(s)) for a given load variable. They illustrate the conditional probability of failure mechanism upon loading [4], without taking the probability of the considered load in to account. These curves can be multidimensional depending on the number of loads considered [4]. Through integration of the fragility curve over the probability density function of the considered load ($f_s(s)$), we can determine the unconditional probability of the considered failure mechanism of the flood defence (see equation 4).

$$P_{f;i} = \int_{r=-\infty}^{r=\infty} \int_{s=-\infty}^{s=\infty} f_{r,s}(r,s)\, dr\, ds = \int_{s=-\infty}^{s=\infty} f_s(s) \cdot F_r(s) ds \qquad (4)$$

Survived loads provide valuable information of the strength of the flood defence, which can be used to reduce uncertainties of the strength of the flood defence and the failure probability. After calculation of the probability of each failure mechanism, we will show how performance observations (survived loads) can be used to update the failure probabilities.

The probability of failure of the considered flood defence section is found by combination of the probability of each failure mechanism, taking interdependencies in to account. The upper and lower bounds of the failure probability are found by assuming independence (upper bound) or complete dependence (lower bound) between failure mechanisms, see equation 5. Finally, the probability of flooding of each scenario can be found by combination of the probability of failure of each flood defence section. Under the assumption of independence between flood defence sections, the probability of flooding of each scenario is calculated with equation 6.

$$\max_{i=1}^{N} P_{f_i} \le P_{f;i} \le 1-\prod_{i=1}^{n}(1-P_{f;i}) \qquad (5)$$

$$P_{f\,scenario} = 1-\prod_{i=1}^{n}(1-P_{f;i}) \qquad (6)$$

2.3 Load uncertainties: canal water level, groundwater level and traffic loads

This section discusses the uncertainties of governing loads on regional flood defences, which consist of hydraulic (e.g. water levels) and traffic loads. The uncertainties of loads on regional flood defences are characterized by extreme value distributions. In our methodology, we used engineering judgment to estimate the probability density functions of load variables for which no data was available for statistical analysis. The continuous probability density functions of these load variables are discretized in a predefined set of plausible load levels with corresponding annual probabilities. The implications of the assumptions made is discussed in section 4.

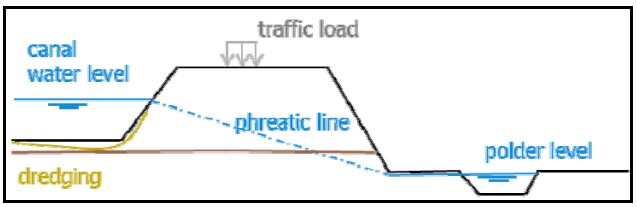

Figure 3. Loads on regional flood defence

2.3.1 Hydraulic loads

The hydraulic loads on regional flood defences consist of the water levels in the canals and the groundwater levels in the regional flood defences. Wave loads are neglected, because the size of waves on canals is negligible (wind waves are small due to the limited fetch on drainage canals). The hydraulic loads both depend on the amount and duration of rainfall in the polder. The following sections discuss the resulting probability distributions of both hydraulic loads.

Water levels in the canals are influenced by inflow from the polder drainage stations and rainfall and by drainage to the surrounding water. The water level in these drainage canals is artificially regulated at a target level above the surrounding polders. This target level is determined by a minimum required drainage capacity in the canal or by more pragmatic reasons, such as a minimum required navigational depth.

The regulated water level is often bounded by a maximum allowed water level, which is defined as the 'drainstop level'. The 'drainstop' ensures that the water level does not exceed the drainstop level. In the Netherlands, the drainstop level has a maximum annual probability of occurrence of 1/100. The difference between the drainstop level and the target water level in the canal is often limited to decimeters. Failure of the drainstop (e.g. because local water authorities neglect or forget to shut down the pumping stations) can result in water levels exceeding the drainstop level.

A Generalized Pareto Distribution (GPD) is fitted through the observations of occurred water levels in the canal to obtain an annual exceedance line of water levels in the canal. This distribution is modified to account for the regulation of water levels through the drainstop, see Figure 4. The water level can follow two exceedance lines: the distribution based on water level observations (f_{GPD}) or the distribution that is capped at the drainstop level ($f_{drainstop}$). Both exceedance lines are combined with equation 8 to obtain a combined distribution f(h) that represents the uncertainty of water levels in the canal. The annual probability of failure of the drainstop [$P_{f;drainstop}$] is estimated by the annual frequency of water level observations that exceeded the 'drainstop level'.

$$f(h) = P_{f;drain\ stop} \cdot f_{GPD} + \left(1-P_{f;drain\ stop}\right) \cdot f_{drain\ stop} \qquad (8)$$

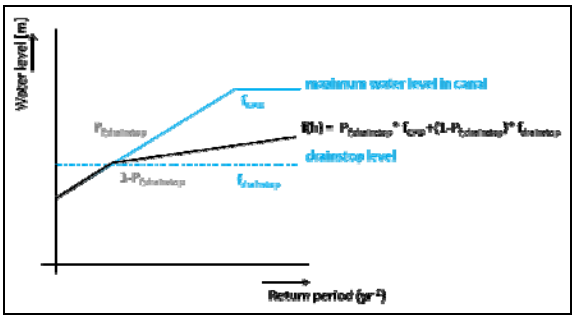

Figure 4. Annual exceedance line of water level in canal

The reliability of this method is largely determined by the amount of water level observations available. An alternative to this empirical method is to determine the failure probability of the drainstop with a human reliability analysis, an example of such an analysis is given in [5,6].

The groundwater level inside the flood defence is influenced by the water level in the canal and the groundwater table inside the polder (Figure 3). The groundwater reduces the effective soil stresses of the soil, which will reduce the stability of the inner slope of the flood defence. The shear strength of the flood defence depends on the phreatic surface. This is a fictive surface where the pore water pressure is under atmospheric conditions (i.e. the pressure head is zero); this level normally coincides with the groundwater table. It is influenced by the water level in the canal, the soil properties of the embankment (e.g. the infiltration capacity) and meteorological aspects such as air moisture, sunshine and rainfall.

To obtain an estimate of annual return periods of the phreatic surface inside a regional flood defence, monitoring of the groundwater table inside the flood defence is required. In absence of this data, we discretized the probability density function of the phreatic surface in a predefined set of plausible load levels, based on an educated guess of the return periods (see Figure 5):

- The low level corresponds with a dry period, which may occur when the water levels in the canal are very low during a period of drought (no rainfall). We assume a probability of 1/100 per year.
- The average level corresponds to an everyday (steady state) situation. We assume a probability of 98/100 per year.
- The high level corresponds to a situation where the flood defence is saturated, which may occur due to an extreme water level in the canal due to extreme rainfall. We assume a probability of 1/100 per year; this corresponding to the probability of a drainstop in polders in the Netherlands.

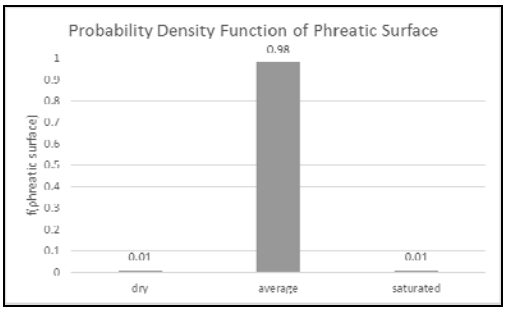

Figure 5. Probability density function of the phreatic surface in a regional flood defence

2.3.2 Traffic loads

Traffic loads may occur permanently, when roads are built on top of regional flood defences, or temporarily, during maintenance of the regional flood defence. The combination of extreme hydraulic and traffic loads can be governing for the stability of the flood defence. Loads on top of flood defences can lead to water overpressure inside the flood defence, which results in a decrease of the shear strength of the flood defence. The extent to which the overpressure develops depends on the soil of flood defence and the duration of the load.

Morales-Napoles [7] studied the influence of dynamic traffic loads on civil structures (e.g. bridges). According to Kwakman [8], moving vehicles have little to no influence on water pressures inside the flood defence. Dynamic forces due to moving vehicles are therefore neglected. Instead, a static top load is taken in to account. Expert elicitation is used obtain an estimate of the uncertainty of the magnitude of this top load. Regional water authority employees responsible for the operation and maintenance of these flood defences were asked to provide estimates of the 5th, 50th and 95th quantiles of the statistical distribution of the traffic load. These estimates were used to generate a triangular distribution of the of the traffic load. More information on the method applied is found in the technical report [3]. The results are presented in Figure 6.

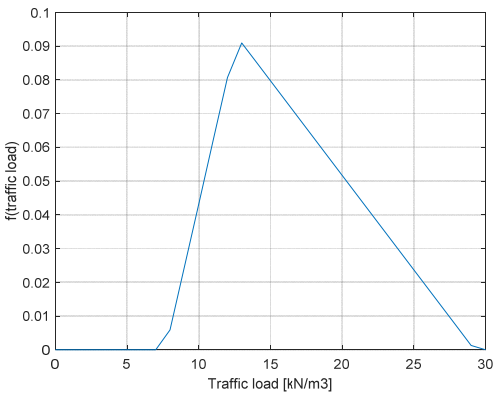

Figure 6. Triangular distribution of traffic load on regional flood defence

The probability of a static traffic load on top of a regional flood defence (Ptrafficload) depends on the local situation, for example if a road is built on top or not. The influence of traffic loads on the stability of the flood defence is illustrated with fragility curves. The probability of inner slope instability of the flood defence will be quantified for a situation with a traffic load ($P_{f;inst|trafficload}$) and without traffic load ($P_{f;inst|\overline{trafficload}}$). The unconditional probability of inner slope instability ($P_{f;inst}$) is found after solving equation 9.

$$P_{f;inst} = P_{f;inst|trafficload} \cdot P_{trafficload} + P_{f;inst|\overline{trafficload}} \cdot P_{\overline{trafficload}}$$
$$\text{with } P_{\overline{trafficload}} = 1 - P_{trafficload} \quad (9)$$

2.4 Governing failure mechanisms

We consider the following failure mechanisms for regional flood defences: overflow, piping and instability of the inner slope. The limit state functions for the governing failure mechanisms are described in the following sections, followed by a description of the methodology used to quantify the (prior) probability of each failure mechanism. Fault tree analysis is used to combine the probability of each failure mechanism and quantify the (upper bound of the) failure probability of the considered dike section, assuming that the failure mechanisms are independent, see equation 6.

2.4.1 Overflow

Overflow occurs when the water levels in the canal (H_w) exceed the retaining height of the flood defence (H_r) and cause erosion of the inner slope. The limit state function ($Z_{overflow}$) takes in to account a critical overflow height (Δh_c) that leads to erosion of the inner slope and ultimately breaching [3]. Monte Carlo simulation is used to determine the probability of overflow, which is defined by the number of negative limit state simulations divided by the total number of simulations. The conditional probability of overflow can be shown in a 2 dimensional fragility curve, dependent on the water level in the canal. The unconditional probability of overflow is found after integrating over the probability density function of the water level.

$$Z_{overflow} = H_r + \Delta h_c - H_w \quad (10)$$

2.4.2 Piping

Piping occurs when the head difference over a flood defence causes seepage (or groundwater flow) through an aquifer below the flood defence, from the canal to the polder behind the flood defence. This may cause uplift of the blanket layer behind the flood defence, after which backward erosion can form pipes in the aquifer under the flood defence. These pipes can undermine the flood defence and ultimately cause failure. The probability of piping depends on the head difference over the flood defence, which is the difference between the water level in the canal (H_w) and the water level in the polder (H_i). The limit state function for piping takes in to account a critical head difference (H_p) over the flood defence, which is calculated with the updated Sellmeijer formula [9].

The water in the drainage canals is not always in direct contact with the aquifer below the flood defence; seepage to the surrounding polder is limited due to te low conductivity of the clayey / peat layers on the bottom of the canals. The intrusion resistance of these layers may impede the development of piping. To account for the intrusion resistance, a variable (H_{ir}) is included in the limit state function of piping that reduces the hydraulic head over the flood defence. The limit state for piping is described by equation 11. The thickness of the blanker layer behind the flood defence is modelled by variable (D_0). The model parameter (m_b) takes in to account model uncertainty.

$$Z_{piping} = m_b \cdot H_p - (H_w - 0.3 \cdot D_0 - H_i - H_{ir}) \quad (11)$$

The amount of intrusion resistance can be reduced (temporarily) due to regular maintenance dredging of these canals (due to removal of the impermeable layers on the bottom of the canals), see Figure 3. Field tests are required to determine the amount (H_{ir}) and probability of reduced intrusion resistance ($P_{f;p|red.int}$) of the bottom layers of the canal. The conditional probability of piping for situations with and without intrusion resistance is determined through Monte Carlo simulation. The influence of the probability of reduced intrusion resistance ($P_{f;p|red.int}$) on the probability of piping is shown in a separate graph (see figures 11 and 12). The unconditional probability of piping ($P_{f;p}$) is found after combining the conditional probability of piping given reduced intrusion resistance ($P_{f;p|red.int}$) and no reduced intrusion resistance ($P_{f;p|\overline{red.int}}$), taking in to account the probability of intrusion resistance ($P_{red.int}$) in equation 12.

$$P_{f;p} = P_{f;p|red.int} \cdot P_{red.int} + P_{f;p|\overline{red.int}} \cdot P_{\overline{red.int}}$$
$$\text{with } P_{\overline{red.int}} = 1 - P_{red.int} \quad (12)$$

The resulting conditional probability of piping is in a 2-dimensional fragility curve that depends on the water level in the canal. The unconditional probability of piping is found after integrating over the probability density function of the water level.

2.4.3 Inner slope instability

Inner slope instability occurs when major soil masses slide of the inner slope of the dike. Instability can be calculated with various methods, which all determine the balance between driving moments (due to horizontal water pressure) and resistance moments (due to shear resistance), for a large number of slip circles of the inner slope. The general limit state function for these methods is described with equation 13.

$$Z_{inner} = M_{resistance} - M_{driving} \quad (13)$$

The Bishop method [10] is used to calculate the stability of the inner slope. Bishop calculates the stability along circular sliding planes. D-Geo Stability is used to determine the probability of inner slope instability. This program uses first order approximation methods (FORM) to determine the conditional probability of inner slope failure depending on a predefined combination of the canal water level, phreatic surface and traffic load. Only slip circles that protrude the crest of the flood defence are taken in to account, as these will lead to breaching of the flood defence. The uncertainties in strength properties are based on the uncertainties used for the primary flood defences [2]. Three separate 2-dimensional fragility curves can be constructed, which show the conditional probability of inner slope instability on each load. The influence of a combination of two loads is shown in 3 separate 3-dimensional fragility curves.

- The unconditional probability of inner slope instability of the considered flood defence section is determined with a probabilistic framework that takes in to account dependence between the considered loads:
- If the loads are independent, the conditional failure probabilities are subsequently integrated over the probability density function of each considered load to obtain the unconditional probability of inner slope instability.
- If the loads are dependent, the unconditional probability of inner slope instability is determined by the dominant load variable. The remaining load variables completely depend on the dominant load variable. The unconditional probability of inner slope instability is found by integration of the conditional probability of inner slope instability over the probability density function of the dominant load variable.

We assume that traffic load on top of the flood defence is independent of the water level and/or the phreatic surface, because these have no direct physical relation. However, the water level and the phreatic surface are both directly influenced by rainfall. The response of both loads to rainfall depends on the considered regional water system and the properties of the considered flood defence section (e.g. the infiltration capacity). The influence of dependence between the water levels and the phreatic surface on the unconditional probability of inner slope instability will be shown in the results, along with an analysis of which load is dominant.

2.5 Using performance observations to update failure probabilities

Posterior analysis (also called Bayesian Updating) is a key element in reliability assessments [9]. Performance observations of a flood defence system can be used to update the (prior) failure probabilities calculated with the methodology explained in the preceding sections. The survival of extreme loads on a flood defence provides information of the strength of the considered flood defence. This information can be used to reduce strength uncertainties and update the computed failure probabilities in a posterior analysis. This section discusses how posterior analysis is used to update the prior probabilities of the failure mechanisms found with the methodology described in the preceding sections.

2.5.1Methodology

Bayes' Rule forms the basis for updating probabilities with evidence of survived loads, see equation 14 where E is the event to be predicted (with the reliability assessment) and the observed event or evidence of the survived load [9]:

$$P(E \mid \varepsilon) = \frac{P(\varepsilon \mid E)\,\mathrm{P(E)}}{P(\varepsilon)} \quad (14)$$

To apply Bayes' Rule in a posterior analysis, we need to distinguish between the type of reliability updating (direct or indirect) to be applied and the type of information (equality or inequality) to be used. A description of the difference between the type of reliability updating and information is included in [9]. Due to its simplicity, we will use direct reliability updating. The information of survived loads used (i.e. the water level the canals) is categorized as equality information, because it can be measured directly.

The posterior analysis largely depends on the availability, accuracy and reliability of data of historically successfully survived loads [11]. The influence of the posterior analyses on the prior failure probability of the flood defence will increase when the survived loads (i.e. the survived water level) approach the maximum loads on the flood defence. The potential influence of a posterior analysis on the prior failure probabilities of regional flood defences is expected to be high, due to the small differences (decimeters) between the average and extreme water levels. Once occurred, these small

differences in water level can be used to reduce the strength uncertainties and update the prior failure probabilities of the flood defence.

The potential influence of the updating procedure also depends on the correlation between the observed survived event and the predicted future event. The updating procedure will have large influence on the prior probability of failure of the flood defence if the strength properties of the observed survived event are highly correlated with the modelled properties of the future event (i.e. if the strength properties of the survived event are similar to those of the future event). In that case, the remaining uncertainty of the reliability analysis lies in the loads.

2.5.2 Potential for considered failure mechanisms

The following section describes the potential of posterior analysis for the governing failure mechanisms in this paper:

- The strength of a flood defence for overflow is determined by the retaining height of the flood defence. The retaining height of a regional flood defence does not change significantly over time, except during reinforcements of the flood defence or due to settlements. If we can exclude reinforcements and settlements during the considered period, we can assume that the retaining height of the survived event is highly correlated to the retaining height of the predicted event. The remaining uncertainty for overflow lies in the load, more specifically the water level in the canals, for which accurate observations are often available. In conclusion, the posterior analysis will have high potential for overflow.
- The strength properties of piping lie in the geotechnical properties of the aquifer under the flood defence (e.g. the permeability, the thickness of the aquifer, the seepage length of the flood defence etc.). The geotechnical properties of the survived event can be assumed to be highly correlated to the geotechnical properties of the predicted event, if we can exclude the possibility of large changes due to excavations or reinforcements. The remaining uncertainty for piping lies in the loads, more specifically the water level in the canals, for which accurate observations are often available. In conclusion, the posterior analysis will also have high potential for piping.
- The strength properties of instability of the inner slope failure mechanism are determined by both the geometrical and geotechnical properties of the flood defence. Similarly to the overflow and piping mechanism, we can assume that these properties are highly correlated between the survived event and the predicted (future) event if we can exclude the possibility of large changes over time. The remaining uncertainty for instability lies in the loads, more specifically the water level in the canals, the phreatic surface inside the flood defence and the magnitude of the traffic loads. The posterior analysis requires accurate information of the combination of these loads during the survived event. The potential of the posterior analysis for the instability failure mechanism largely depends on the availability of information of the occurred phreatic surface and traffic load in combination of the observed extreme water level during the survived event.

3 Case Study "Heerhugowaard"

3.1 Case description

The methodology was applied to a system of regional flood defences surrounding a polder in the western part of the Netherlands. The studied polder, named the 'Heerhugowaard', is governed by the Dutch water authority called Hoogheemraadschap Hollands Noorder Kwartier (HHNK). It is surrounded by two large drainage canals that drain excess water from the polders to the North Sea: the Schermer and VRNK canal. The polder is protected from flooding by a system of regional flood defences with a total length of 32 kilometers, which is divided in six flood scenarios based on flood propagation simulations made by the water authority. Each flood scenario consists of a group of flood defence sections, these are illustrated in Figure 7. The locations of four pumping stations along the regional flood defence system is also shown.

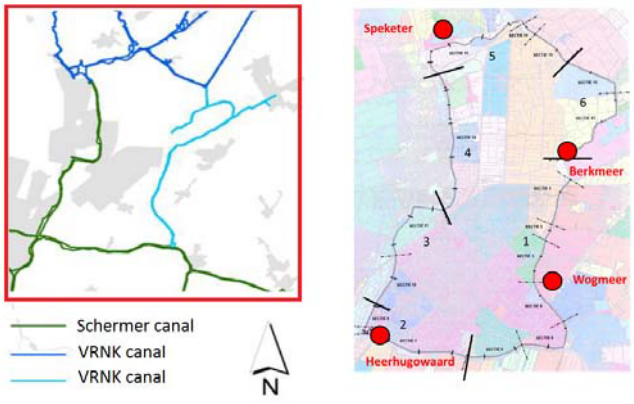

Figure 7. Overview of the Heerhugowaard polder surrounded by the Schermer and VRNK canals (left) and plan view of schematization of regional flood defence system including the drainage stations (Lendering et al. 2015)

3.2 Load uncertainties

This section describes the loads taken in to account in the case study. General probability density functions were derived in section 2.3 for the phreatic surface and the traffic loads on regional flood defences. The annual exceedance lines of the canal water level are determined using water level observations in the Schermer and VRNK canal, based on the methodology derived in section 2.3.1. Figure 8 shows the resulting fit for the the Wogmeer station in the VRNK canal.

The drainstop level (MBP) of each canal is shown Figure 9. The probability of drainstop failure is estimated using the frequency of exceedance of the drainstop level, according to the methodology explained in section 2.3.1. This resulted in a probability of drainstop failure of 1/9 per year for the VRNK canal. The combined exceedance line of the water level in the VRNK canal is shown in Figure .

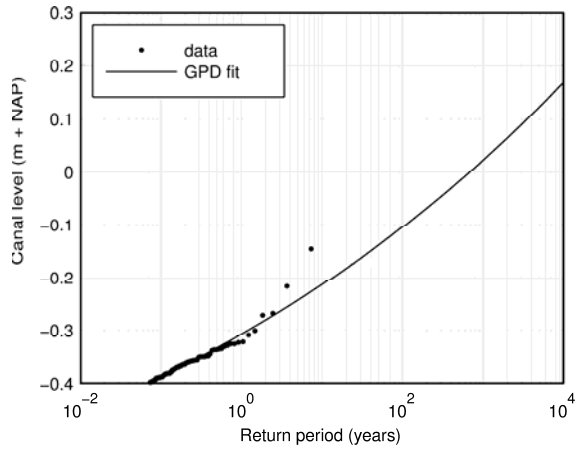

Figure 8. Wogmeer station water levels

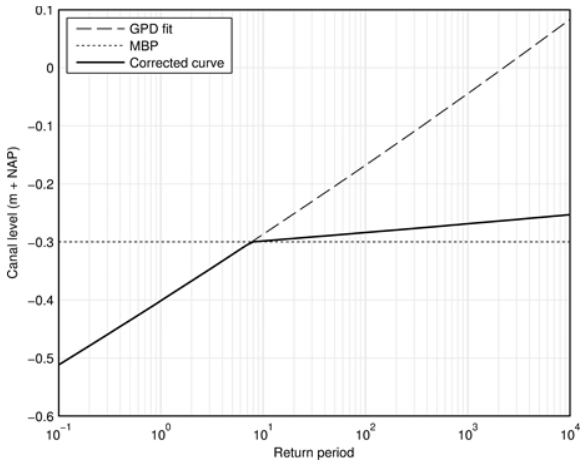

Figure 9. Combined exceedance line of the Wogmeer station

3.3 Results

This paragraph discusses the results of the failure probability assessment for the first scenario of the case study (scenario 1). The data used for the calculations can be found in the technical report (Lendering et al. 2015). As a first approximation, the failure probability of the weakest section (section 4) of the considered flood scenario (scenario 1) is used to determine the probability of flooding for the scenario (e.g. the section with the lowest retaining height is used to determine the probability of overflow). In a full probabilistic analysis, the probability of failure of all sections within one flood scenario need to be combined to obtain the probability of flooding of the considered scenario.

3.3.1 Overflow

The strength for overflow is determined by the retaining height of the flood defence. The fragility curve and probability of overflow are determined with Monte Carlo simulation. The fragility curve is shown in Figure 10. The probability of overflow of the considered flood scenario is negligible, because the retaining height of the considered flood defence lies well above the water levels in the canal and corresponds to water levels with return periods below 1/100.000 per year. This is mainly the result of very low probabilities of drainstop failure (which results in very low probabilities of extreme water levels). No posterior analysis is performed due to the low probability of overflow.

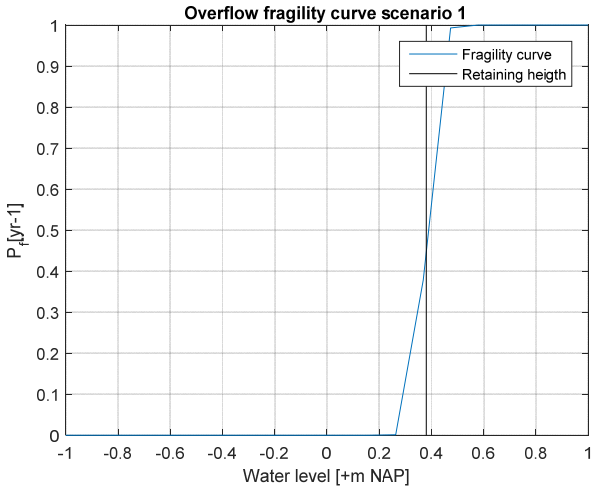

Figure 10. Overflow fragility curve of flood scenario 1

3.3.2 Piping

The prior probability of piping (i.e. the probability of piping before posterior analysis) depends on the amount (H_{ir}) and probability of reduced intrusion resistance ($P_{f;p|red.int}$). Monte Carlo simulation is used to determine the conditional probability of piping and the corresponding fragility curve. The probability of piping increases with increasing probability of reduced intrusion

resistance ($P_{red.int}$)), see Figure 11. From the graph can be concluded that the conditional probability of piping varies between a probability of 0.005 and 0.034 per year, depending on the probability of reduced intrusion resistance. Field tests are required to determine the amount and probability of reduced intrusion resistance of the bottom layers of the canal.

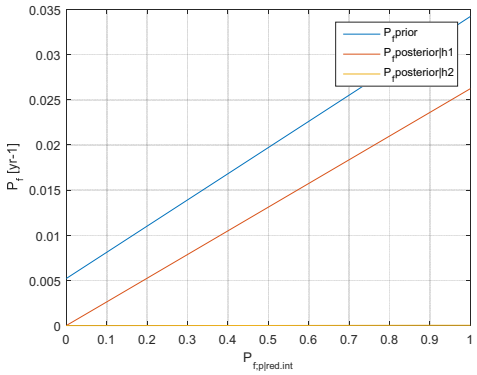

Figure 11. Probability of piping of conditional on the probability of reduced intrusion resistance

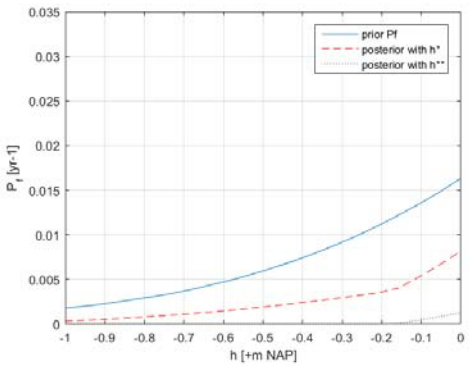

Figure 12. Probability of piping of conditional on the water levels

The range, and especially the upper bound, of the conditional probability of piping is considered to be rather high, given the fact that no signs of piping (e.g. heave or uplifting) in the considered regional flood defence system during the last decades. Reliability updating is used to further optimize the probability of piping, given evidence of survived loads. The highest observed water level in the canal along flood scenario 1 is used in the posterior analysis. Due to lack of information of dredging depths during the observed extreme water level, we assume that the impermeable layer on the bottom of the canal was present during the survived load. The combination of the survived water level and the presence of intrusion resistance is defined as load case h1 and leads to a small reduction of the hydraulic head over the flood defence. This reduction is in the same order of magnitude as the difference between the average water level and the maximum observed water level. The survival of load case h1 results in a reduction of the probability of piping ($P_{fposterior|h1}$) to a range of <10-5 and 0.026 per year, as can be seen in Figure 12.

Suppose that that the impermeable layers on the bottom of the canal were removed right before the survived load occurred, resulting in reduced intrusion resistance. The hydraulic head during this (fictive) load case, defined as h2, is significantly higher than the average hydraulic head over the flood defence (in the order of several meters) in daily circumstances, due to the reduced intrusion resistance. The survival of this (fictive) load case can prove that the considered flood defence can survive significantly larger loads than it is exposed to on a daily basis. The conditional probability of piping given load case h2 ($P_{fposterior|h2}$) is calculated and included in Figure 12. This probability reduced is smaller than 10-5 per year, which is more realistic considering the absence of signs of piping in the regional flood defence. This (fictive) load case can be created by removing the impermeable layer on the bottom of the canal and raising the water level in the canal.

An estimate of the probability of reduced intrusion resistance is required to calculate the probability of piping with equation 12. The Schermer and VRNK canals are dredged every year. The probability of accidental removal of the impermeable layer during dredging (due to human error) is estimated at 1/10 per dredging activity, resulting in a probability of 1/10 per year for reduced intrusion resistance. The probability of piping for flood scenario 1 can now be calculated using equation 12. The posterior probability of piping given load case h1 is used, because we cannot exclude the possibility of intrusion resistance during the survived load. This results in a probability for piping of ($0.026 \cdot 0.9 + 10^{-5} \cdot 0.1$) 0.0026 per year. This probability is dominated by the probability of piping given reduced intrusion resistance and could be reduced further if the probability of reduced intrusion resistance due to maintenance dredging is reduced. The fragility curves for the conditional probability of piping in the prior, posterior given h1 and posterior given h2 analyses are also shown in Figure 12. Comparison of the conditional probability of piping on the probability of reduced intrusion resistance and the occurring water level shows that the probability of intrusion resistance has more influence on the probability of piping.

3.3.3 Inner slope instability

The stability of the inner slope depends on three loads: i) the water levels in the canal, ii) the phreatic surface in the flood defence and iii) the traffic load on top of the flood defence. The conditional probability of inner slope instability is calculated with D-Geo Stability for several combinations of these loads, assuming independence between every load. Figure 13 contains fragility curves for every load after integration over the remaining loads. The figures show that the phreatic surface has the largest influence on the stability of the inner slope, followed by the traffic load.

The probability of inner slope instability depends on the correlations between the considered loads. In section 2.4.3, we argued that the traffic load is independent of the hydraulic loads. The correlation between the canal water level and the phreatic surface depends on the considered physical system. We assume that the water levels in the canal and the phreatic surface are positively dependent, because both are influenced by rainfall and higher water levels in the canals will cause an increase of the phreatic surface of the flood defence. The fragility curves in Figure 13 show that the probability of inner slope instability is influenced significantly by the phreatic surface. Moreover, the figure shows that variations of the water level in the canal do not influence the probability of inner slope instability significantly. Given these observations, we conclude that the phreatic surface of the flood defence is the dominant hydraulic load. The probability of inner slope instability given positive dependence between the water level and the dominant phreatic surface is included in Table 1, depending on the presence of traffic loads. For comparison purposes, the probability of inner slope instability given independence between the hydraulic loads is also included.

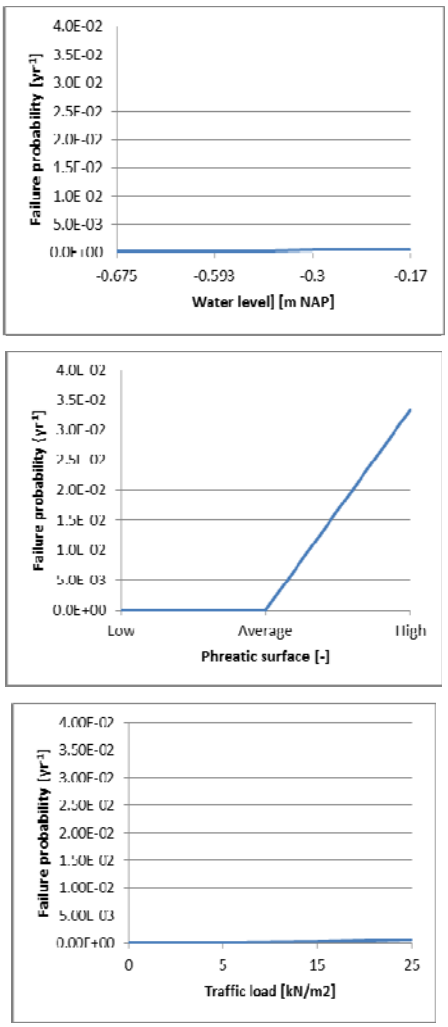

Figure 13. Fragility curves for inner slope instability depending on three loads: water level (top), phreatic surface (middle) and traffic load (bottom)

Dependence between water level and phreatic surface	$P_{f;inst\|\overline{trafficload}}$ [yr-1]	$P_{f;inst\|trafficload}$ [yr-1]	$P_{f;inst}$ [yr-1]
Independent	1.3 *10-4	3.3*10-4	2.3*10-4
Dependent	1.9 *10-4	4.9*10-4	3.4*10-4

Table 1. Resulting failure probabilities for instability of the inner slope of scenario 1

The unconditional probability of inner slope instability is found by solving equation 9, assuming a probability of traffic loads ($P_{trafficload}$) of 1/2 per year. Posterior analysis were not performed for the instability failure mechanism, due to lack of accurate information of the phreatic surface and traffic load during the observed water levels. Engineering judgment could be used to make an educated guess of the level of the phreatic surface and traffic load during the observed water level, to demonstrate the potential of the posterior analyses for the instability failure mechanism.

3.3.4 Probability of flood scenario

The probability of each failure mechanism for all flood scenarios in the case study are shown in Table 2. These failure probabilities are combined, assuming independence between the governing failure mechanisms, to obtain an estimate of the probability of each flood scenario according to equation 6 (see last column). The resulting probability of flooding in the considered polder varies between 1/20 and 1/350 per year.

Flood scenario	$P_{f;overflow}$ [yr^{-1}]	$P_{f;piping}$ [yr^{-1}]	$P_{f;inst}$ [yr^{-1}]	P_f [yr^{-1}]
1	$< 10^{-5}$	$2.64 *10^{-3}$	$3.4*10^{-4}$	0.00028 (1/380)
2	$< 10^{-5}$	$4.78 *10^{-2}$	$1.2*10^{-4}$	0.05 (1/20)
3	$< 10^{-5}$	$8.24 *10^{-4}$	$3.5*10^{-3}$	0.004 (1/250)
4	$< 10^{-5}$	$1.42 *10^{-2}$	$< 10^{-5}$	0.014 (1/70)
5	$< 10^{-5}$	$3.60 *10^{-3}$	$2.4*10^{-4}$	0.004 (1/250)
6	$< 10^{-5}$	$5.00 *10^{-3}$	$< 10^{-5}$	0.005 (1/200)

Table 2. Resulting probability of flooding for every scenario of the case study

We conclude that the probability of failure is governed by the probability of piping and instability of the inner slope. The uncertainty of the water levels proved to be negligible compared to the uncertainty of the reduced intrusion resistance, traffic loads and the phreatic surface of the regional flood defence.

4. Implications

Engineering judgment was used to estimate the probability density functions of load variables for which no data was available for statistical analysis. The implications of these assumptions are discussed in this section.

A method was developed to determine the combined probability of exceedance line of water levels in a canal, based on an empirical distribution of observed water levels. The probability of failure of the drainstop was estimated by the amount of independent water level peaks exceeding the drainstop level. The reliability of this method is largely determined by the amount of water level observations available. An alternative to this empirical method is to determine the failure probability of the drainstop with a human reliability analysis, an example of such an analysis is given in (Lendering et al. 2015; Kirwan 1996).

In absence of data of the occurring phreatic surface, influenced by the canal water level and rainfall, the probability density function of the phreatic surface was discretized in a predefined set of plausible load levels, based on an educated guess of their return period. Monitoring of the phreatic surface is recommended to assess whether or not the assumed return periods are accurate. Data of the occurring phreatic surface, influence by the canal water levels, will also provide insight in the dependence between these loads. In the considered case study of the Heerhugowaard, the canal water levels proved to have little effect on the probability of instability of the inner slope. This may not be the case in all considered systems.

The magnitude and probability of the traffic load on top of regional flood defences was estimated with expert elicitation. The probability of instability of the inner slope was determined assuming a probability of traffic loads of 1/2 per year. The consulted experts had different views on whether or not traffic should be allowed on the considered flood defences, because of the considerable influence of traffic loads on the probability of failure. The assume probability of traffic loads requires further investigation.

5. Conclusions and recommendations

This paper proposed a methodology to quantify the probability of flooding of regional flood defence systems, based on the probabilistic methods developed for the primary flood defence systems in the Netherlands. The application to the regional flood defence system required several additions to the methodology, to account for regulation (and drainstop) of the water levels in the canals, the possibility of (reduced) intrusion resistance on the bottom of the canal due to maintenance dredging, the probability of traffic loads on top of a regional flood defence and the influence of dependence between the canal water levels and the phreatic surface of a regional flood defence. In addition, reliability updating is used to demonstrate the (high) potential for updating the probability of failure of regional flood defences based on performance observations.

The proposed methodology was applied to a case study of a regional flood defence system in the Netherlands. The probability of flooding of the considered system was determined for three governing failure mechanisms: overflow, piping and instability. The probability of overflow largely depends on the probability of drainstop failure. For piping, the probability of failure is largely determined by the probability of (reduced) intrusion resistance of the bottom layer of the canal. A posterior analysis demonstrated the ability to reduce the probability of piping using performance observations. This potential was high due to the small differences between the daily water levels and extreme water levels in the canal. The posterior analysis can be used more effectively by testing the stability for piping given a certain (extreme) water level and reducing the intrusion resistance on the bottom of the canal.

The probability of instability of the inner slope largely depends on the uncertainty in the phreatic surface and the probability of traffic loads. Monitoring of the phreatic surface is recommended to assess whether or not the assumed return periods are accurate. Posterior analysis were not performed for the instability failure mechanism, due to lack of accurate information of the phreatic surface and traffic load during the observed water levels. However, a method was proposed which can be used to investigate whether or not posterior analyses can have high potential for updating instability failure probabilities.

Overall, we conclude that the proposed methodology can be used to determine the probability of flooding of a regional flood defence system. By doing so, the methodology contributes to improving flood risk management in regional flood defence systems, for example by using cost benefit analyses to prioritize flood risk reduction measures based on their effect on the probability of flooding of the considered system.

6. Acknowledgements

The authors would like to express their gratitude to the STOWA, which is the research department of the Dutch water authorities, for providing the necessary resources to undertake this project. In addition, all those involved from the regional water authority HHNK are thanked for their cooperation during the project. Finally, Professor S.N. Jonkman is thanked for his useful comments and insights during the extent of the project. The authors acknowledge that there are no potential sources of conflict of interest in this paper.

7. References

1. Vrijling, J.K., 2001. Probabilistic design of water defense systems in The Netherlands. *Reliability engineering & system safety,* **74(3)**, 337–344. Available at: http://www.sciencedirect.com/science/article/B6V4T
2. Jongejan, R., Maaskant, B. & Horst, W. ter, (2013). The VNK2-project: a fully probabilistic risk analysis for all major levee systems in the Netherlands. *IAHS ..., 2005*. Available at: http://www.hkvconsultants.de/documenten/The_VNK2_project_a_fully_probabilistic_risk_etc_BM_FH(2).pdf [Accessed May 16, 2014].
3. Lendering, K.T., Kok, M. & Jonkman, S.N., 2015. Flood Risk Regional Flood Defences, Amersfoort.
4. Vorogushyn, S., Merz, B. & Apel, H., 2009. Development of dike fragility curves for piping and micro-instability breach mechanisms. *Natural Hazards and Earth System Science*, **9**, 1383–1401.
5. Lendering, K.T., Jonkman, S.N. & Kok, M., 2015. Effectiveness of emergency measures for flood prevention. *Journal of Flood Risk Management, ICFM6(Special Issue)*.
6. Kirwan, B., 1996. The validation of three Human Reliability Quantification techniques—THERP, HEART and JHEDI: Part 1—technique descriptions and validation issues. *Applied ergonomics,* **27(6)**, 359–73. Available at: http://www.ncbi.nlm.nih.gov/pubmed/15677076 [Accessed November 20, 2013].
7. Morales-nápoles, O. & Steenbergen, R.D.J.M., 2014. Large-Scale Hybrid Bayesian Network for Traffic Load Modeling from Weigh-in-Motion System Data. *Journal of Bridge ...,* 1–10. Available at: http://ascelibrary.org/doi/abs/10.1061/(ASCE)BE.1943-5592.0000636 [Accessed January 21, 2015].
8. Kwakman, L., 2013. Vervolgonderzoek schematisering verkeersbelastingen op kades, Hoorn.
9. Schweckendiek, T., 2014. On Reducing Piping Reliabilities: A Bayesian Decision Approach. Delft University of Technology.
10. Bishop, A.W., (1955). The use of the slip circle in the stability analysis of slopes. *Geotechnique,* **5**, 7–17.
11. Stowa, 2009. Technisch Rapport Actuele sterkte van dijken, Amersfoort.